

## Application of modified coriander seeds as biomaterial for removal of fluoride from aqueous media

Fatemeh Moradi<sup>a</sup>, Sahar Shirmohammadi<sup>b</sup>, Ahmad Zarei<sup>c</sup>, Mohsen Rezaei<sup>d,\*</sup>

<sup>a</sup>Department of Environmental Health Engineering, School of Public Health, Tehran University of Medical Sciences, Tehran, Iran, email: f.moradi590@gmail.com

<sup>b</sup>Department of Environmental Health Engineering, Faculty of Public Health, Ardabil University of Medical Sciences, Ardabil, Iran, email: Shsahar602@gmail.com

<sup>c</sup>Department of Environment Health Engineering, Faculty of Health, Social Determinants of Health Research Center, Gonabad University of Medical Sciences, Gonabad, Iran, email: a.zarei.tums@gmail.com

<sup>d</sup>Department of Chemistry, University of Copenhagen, Copenhagen, Denmark, email: mohsen@chem.ku.dk

Received 6 June 2019; Accepted 26 October 2019

---

### ABSTRACT

The presence of fluoride ion above the permissible limits in drinking water can be a well-recognized risk factor for human health. Fluoride ion adsorption from aqueous media on modified coriander seeds, as a low-cost biomaterial, was investigated. The influence of adsorption parameters such as contact time, initial pH, adsorbent dosage, initial fluoride concentration, and temperature was studied. The results showed that the sorption process was influenced by these variables. Fluoride adsorption was confirmed by scanning electron microscopy. The Langmuir model has a good correlation to the adsorption data. Also, the dimensionless constant separation factor ( $R_L$ ) values verified a highly favorable adsorption. The value of activation energy ( $580 \text{ kJ mol}^{-1}$ ) represented that the sorption process is chemical. Based on the kinetic studies, the pseudo-second-order model yielded a better fit to experimental data, showing a chemisorption process. The adsorption process of fluoride removal onto modified coriander seeds was endothermic. Coriander seeds showed high adsorption potential and can be applied as a low-cost bioadsorbent for the rapid removal of fluoride ions from aqueous solution.

*Keywords:* Fluoride; Adsorption; Modified coriander seeds; Aqueous solutions

---

### 1. Introduction

Nowadays, human activities and natural processes have polluted many water resources [1,2]. Fluoride is extensively applied in various industries including aluminum electrolysis, ceramics, cement, glass, semiconductor, steel, pharmaceutical, etc. [3]. Besides the natural sources for discharge into groundwater, different industrial sources are also contributing to ground and surface water pollution to fluoride that have a wide range of fluoride from 10 to

1,000  $\text{mg L}^{-1}$  [4]. The generation and discharge of a large amount of fluoride-containing effluents have led to the continuous increase of the concentration of fluoride ion in rivers, lakes, and streams, which seriously pollutes the environment [5,6]. Naturally, fluoride is widely released into the groundwater by the dissolution of various minerals, for example, topaz, fluorite, biotites and fluorine-containing rocks such as granite, basalt, syenite, and shale [7]. A little amount of fluoride ions in drinking water has a beneficial health effect on human especially to children dental caries

---

\* Corresponding author.

[8]. On the contrary, long-term excessive fluoride intake [9] is a well-recognized risk factor in causing several diseases such as dental and skeletal fluorosis, osteoporosis, arthritis, brittle bones, bladder cancer, infertility, brain damage, Alzheimer's syndrome, and thyroid disorder [10]. Dental and skeletal fluorosis is a major public health concern in different countries: for example, Mexico, India, Iran, Africa, and the United States [11]. The World Health Organization (WHO) has recommended a fluoride guideline range of 0.5–1.5 mg L<sup>-1</sup> for drinking water. It is estimated that more than 200 million people in the world consume drinking water with fluoride concentrations exceeded the WHO guideline [12]. Different methods for defluoridation of water have been applied including precipitation and coagulation processes (with ferric, activated alumina, alum, and calcium), ion exchange, membrane processes and electro dialysis [13]. However, these methods have high operational and maintenance costs, high sludge production and require a complicated procedure. The coagulation methods have generally been found effective in defluoridation, but they are unable to reduce the fluoride concentration to target levels. Moreover, membrane processes do not require chemical materials injection however these are costly to operate and also have pretreatment, fouling and scaling problems. The main disadvantage related to the electrochemical techniques is operational and maintenance costs [14].

Among different technologies, the adsorption seems to be a more attractive method for the removal of fluoride from water in terms of cost, simplicity of design and operation [15,16]. Also, greater accessibility and availability of a wide range of adsorbents are considered as the important advantages of these technologies [17,18]. However, in this method achieving a high efficiency often requires the adjustment and readjustment of pH, and some common water ions can interfere with fluoride adsorption. Adsorption depends on the transmission of adsorbate (ions) to the surface of a solid material in fluid, where they bond with the solid material surface or by weak intermolecular forces is held [19]. The removal of fluoride by adsorption methods has been widely studied in recent years, however, interest is growing in the use of low-cost adsorbent including biological [20], waste [21] and natural chemical adsorbents [22].

This paper has focused on investigating the use, adsorption isotherm and kinetics of *Coriandrum sativum* seeds (coriander) as a low-cost natural material at variable initial fluoride concentration. *Coriandrum sativum* is from the family of *Apiaceae* (*Umbelliferae*) and cultivated during all seasons. Seeds of the plant have been widely used in most countries due to its clinical beneficial effects on the human [23].

Pretreatment of solid adsorbent to remove soluble organic compounds and enhance efficiency of impurities adsorption such as fluoride have been performed by many researchers [24]. Recently, different kinds of modifying agents were used for the above-mentioned purposes such as base solutions, mineral, and organic acid solutions, oxidizing agents, etc. The application of a strong dehydrating agent like sulfuric acid (H<sub>2</sub>SO<sub>4</sub>) can have a significant effect on the surface area of the adsorbent by increasing the micropores area [25]. In the present study, we applied coriander seeds activated with sulfuric acid for fluoride removal and investigated the effect of different parameters including

pH, adsorption time, initial concentration of fluoride and adsorbent dosage on the fluoride adsorption efficiency in the synthetic aqueous solution.

## 2. Materials and methods

### 2.1. Preparation of the adsorbent

Coriander seeds were washed with distilled water to remove dust and dirt. Then, it was dried in an oven at 70°C for 12 h, cooled in room temperature, crushed, sieved to the particle size of 2 mm and kept in sulfuric acid 1 N for 12 h for activation. Finally, the resulting product was rinsed with distilled water to wash the remaining acid and dried again at the same temperature for 12 h. The modified seed was stored in airtight stainless steel containers for the experiments.

### 2.2. Preparation of adsorbate solution

Stock solution of fluoride (100 mg L<sup>-1</sup>) was prepared by dissolving an exact amount of NaF salt (purchased from Merck Co., Germany) in double deionized water. All the desired concentrations of fluoride ranging from 5 to 30 mg L<sup>-1</sup> were prepared from the stock solution of fluoride during the experiments.

### 2.3. Adsorption procedure and experiments

Adsorption studies were carried out in batch condition in three different phases which include: determination of optimal pH, optimal adsorbent dosage and appropriate adsorbate concentration. Various amounts of the adsorbent (2–8 g L<sup>-1</sup>) were individually added to conical flasks containing 250 mL fluoride solution with concentrations of 5–30 mg L<sup>-1</sup> and adjusted pH values of 3–11. Each mixture then was shaken (180 rpm) at room temperature (20°C) for 90 min. At each defined interval time of ranging from 2 to 90 min, an adequate volume of the solution was sampled and filtered using Whatman filter paper 0.42 micron. After dilution with distilled water to a final volume of 8 mL and adding 2 mL of sodium 2-(p-stilfophenylizo)-1, 8-dihydroxy-3, 6-naphthalenedisulfonate (SPDNS), final concentration of fluoride was determined in the filtrate by UV-Vis spectrophotometer at λ<sub>max</sub> of 580 nm (DR-5000-HACH LANGE Co., Germany). The method for the analysis of fluoride is described in detail in Standard Methods for the Examination of Water and Wastewater [26].

The amount of fluoride adsorbed by the adsorbent was calculated by following equation [27,28]:

$$q_e = \frac{(C_0 - C_e) \times V}{M} \quad (1)$$

where  $q_e$  is the amount of fluoride adsorbed (mg g<sup>-1</sup>),  $C_0$  and  $C_e$  are the initial and residual concentrations of fluoride at equilibrium (mg L<sup>-1</sup>), respectively.  $V$  is the volume (L) of the solution and  $M$  is the weight of adsorbent (g) used.

### 2.4. Characterization of adsorbent

Scanning electron microscopy (SEM) (LEO 1430 VP, Germany) was used to study the surface morphology of

adsorbent before and after adsorption at an accelerating voltage of 20 kV. Fourier transform infrared spectroscopy (FTIR) (PerkinElmer Life and Analytical Sciences, CT, USA) was utilized to determine the presence of functional groups on the adsorbent, before and after adsorption. Spectra were recorded in the range of 400–4,000 wavenumbers ( $\text{cm}^{-1}$ ).

### 2.5. Determination of point of zero charge ( $\text{pH}_{\text{pzc}}$ )

To determine the point of zero charge ( $\text{pH}_{\text{pzc}}$ ) of the adsorbent, 250 mL distilled water was added to each of the 6 flasks. HCl 0.1 M and NaOH 0.1 M were used to adjust the  $\text{pH}_{\text{in}}$  of these solutions. 0.5 g adsorbent was then added to each flask and stirred by a shaker. After 24 h the final pH ( $\text{pH}_{\text{f}}$ ) of the solutions was recorded. Finally, the difference between the  $\text{pH}_{\text{in}}$  and  $\text{pH}_{\text{f}}$  values were plotted against  $\text{pH}_{\text{in}}$ . The point of intersection of the resulting curve with the horizontal axis gave the  $\text{pH}_{\text{pzc}}$  [29].

## 3. Results and discussion

### 3.1. Characterization of adsorbent

#### 3.1.1. SEM micrographs

The SEM micrographs of modified coriander seeds modified with  $\text{H}_2\text{SO}_4$  before and after adsorption experiments

are depicted in Figs. 1a–d, respectively. It is clear from Figs. 1c and d that the morphology of the surface has slightly changed after fluoride adsorption. Adsorbed fluoride on the surface of the seeds can be seen in the form of white patches, confirming probably precipitation of fluoride [30,31].

#### 3.1.2. FTIR spectra

Figs. 2a and b show the FTIR spectra of modified coriander seeds. As shown in Fig. 2a the presence of the hydroxyl group ( $-\text{OH}$ ), related to the peak of  $3,294 \text{ cm}^{-1}$ , is due to inter and intramolecular hydrogen bonding or  $-\text{NH}$  stretching vibration related to secondary amides. The  $-\text{OH}$  stretching vibrations is attributed to free hydroxyl groups ( $-\text{OH}$ ) and banded carboxylic acids. The adsorption at  $2,929 \text{ cm}^{-1}$  indicates asymmetric C–H stretching vibration of aliphatic acids. The peak at  $2,855 \text{ cm}^{-1}$  confirms the presence of symmetric stretching vibration of  $\text{CH}_2$  due to C–H bonds belonging to aliphatic acids. The stretching vibration of  $\text{C}=\text{O}$  due to non-ionic carboxyl groups or esters was verified by peak at  $1,747 \text{ cm}^{-1}$ . The absorption at  $1,635 \text{ cm}^{-1}$  is caused by a stretching peak related to  $\text{C}=\text{C}$  groups.  $1,533 \text{ cm}^{-1}$  can be attributed to nitroso ( $\text{N}=\text{O}$ ) groups. The methylene group has a characteristic bending adsorption of approximately  $1,458 \text{ cm}^{-1}$ . The absorption at band  $1,379 \text{ cm}^{-1}$  is ascribed to the symmetric stretching of  $-\text{COO}$ . The band at about

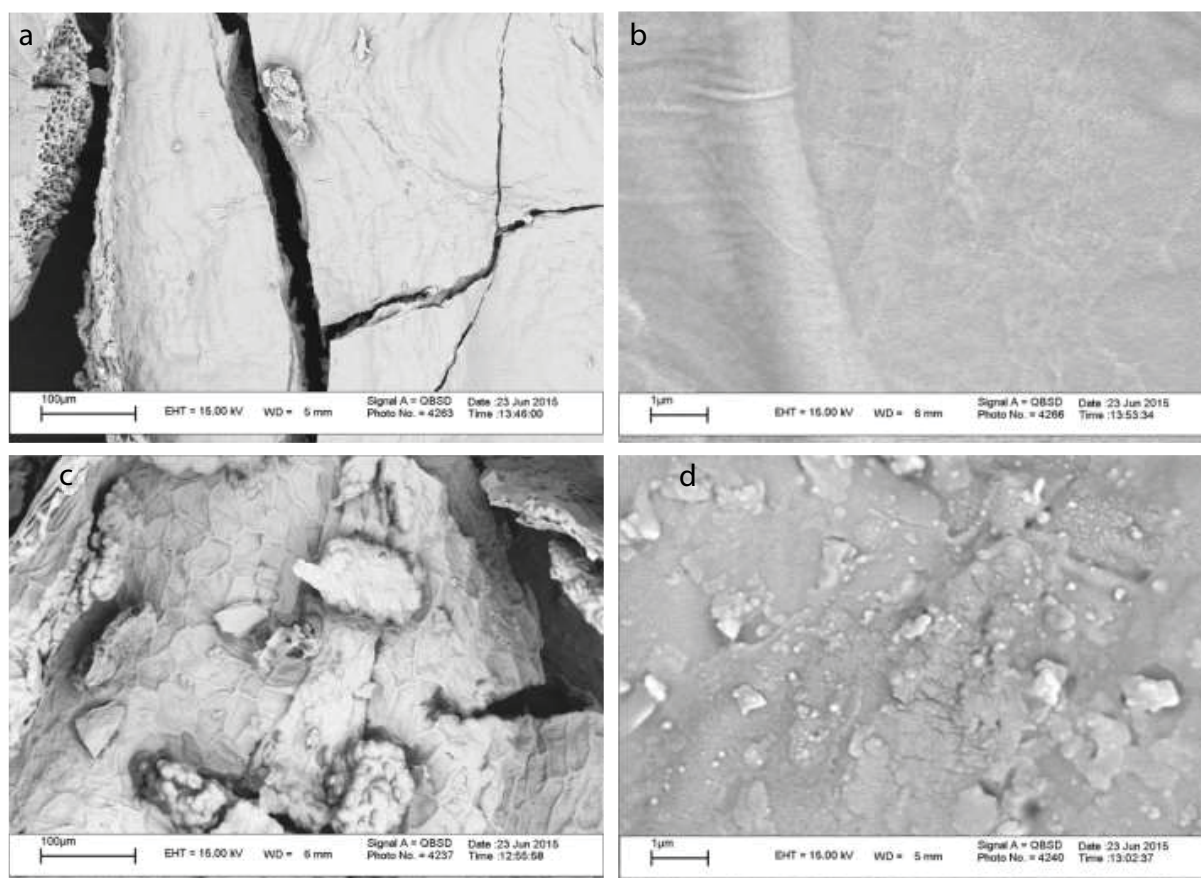


Fig. 1. Surface morphology of  $\text{H}_2\text{SO}_4$ -modified coriander seeds ((a) magnification of 500 $\times$  and (b) 30,000 $\times$ ) and  $\text{H}_2\text{SO}_4$ -modified coriander seeds loaded with fluoride ((c) magnification of 500 $\times$  and (d) 30,000 $\times$ ).

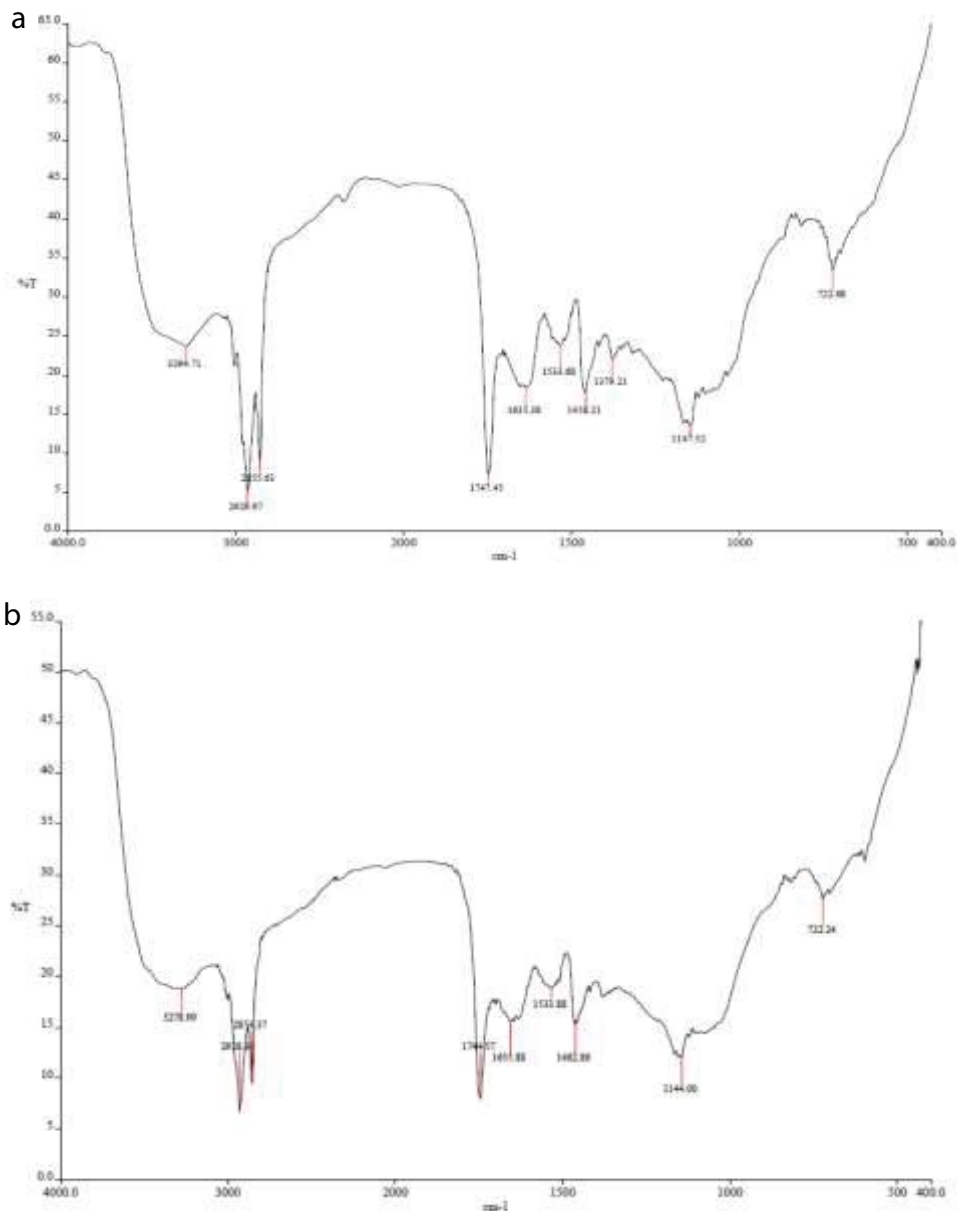


Fig. 2. FTIR spectra of coriander seeds (a) before and (b) after fluoride adsorption.

$1,147\text{ cm}^{-1}$  is due to groups of nitrogenous such as aliphatic amines. It should also be noted that S=O has a symmetric stretch (strong) near the wavenumber. The bands at  $722\text{ cm}^{-1}$  can be related to C–H deforming or  $\text{CH}_2$  rocking [32]. FTIR spectra of the seeds was shifted from the peaks at about 3,294; 2,929; 2,855; 1,747; 1,635; 1,533.7; 1,458; 1,379; 1,147 and  $722.7\text{ cm}^{-1}$  to 3,278; 2,928; 2,854; 1,744; 1,655; 1,533.9; 1,462; 1,144; and  $722.2\text{ cm}^{-1}$ , respectively.

### 3.2. Determination of pH point of zero charge ( $\text{pH}_{\text{pzc}}$ )

The pH point of zero charge ( $\text{pH}_{\text{pzc}}$ ), is a concept related to the phenomenon of adsorption that describes the condition of adsorption when the electrical charge density on a surface is zero. It determines how easily a substrate can

adsorb potentially harmful ions. When the pH is lower than the  $\text{pH}_{\text{pzc}}$  value, the adsorbent surface is positively charged and attracts anions. Conversely, in above  $\text{pH}_{\text{pzc}}$  the surface is negatively charged and attracts cations [29]. As it is shown in Fig. 3, in this study,  $\text{pH}_{\text{pzc}}$  of the Coriander seed modified with sulfuric acid was obtained about 6.6.

### 3.3. Effect of operating parameters

#### 3.3.1. Effect of adsorption time

Fig. 4 shows the effect of adsorption time on the adsorption efficiency (data is not shown) and adsorption capacity of fluoride. The adsorption time was applied from 2 to 90 min at an initial pH of 7, the adsorbent dosage of  $2\text{ g L}^{-1}$  and initial fluoride concentration of  $5\text{ mg L}^{-1}$ . It was observed that

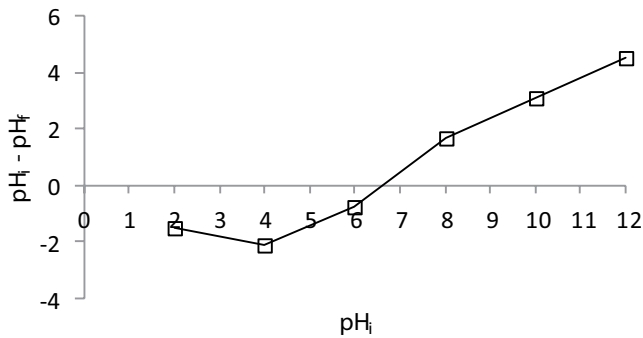


Fig. 3. Point of zero charge: coriander seeds, 0.5 g; temperature, 20°C; and solution volume 250 mL.

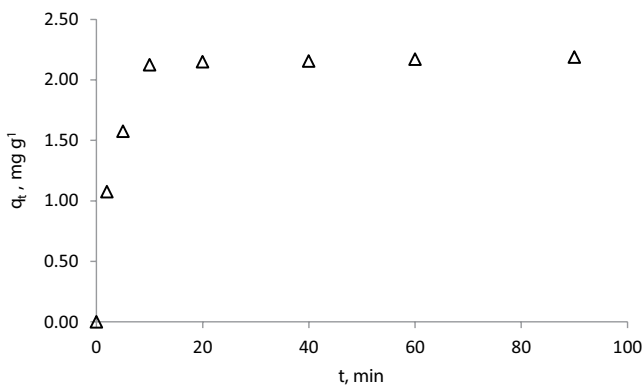


Fig. 4. Effect of adsorption time on the adsorption amounts of coriander seeds: initial fluoride concentration, 5 mg L<sup>-1</sup>; initial pH, 5.0; temperature, 20°C; and adsorbent dose, 2 g L<sup>-1</sup>.

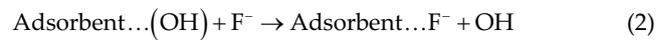
the efficiency and adsorption capacity of fluoride increased gradually with increasing adsorption time and reached a plateau after 10 min of reaction. After that time, the efficiency and capacity no further changed significantly. Thus, the adsorption time of 10 min was the equilibrium point of adsorption. Therefore, the fluoride adsorption occurred rapidly. In most studies, capacity and absorption efficiency was increased by time [33]. However, the equilibrium time of the present study was lower than those of other studies, and it can be considered as an important advantage of the coriander seeds. Also, it can be found from Fig. 4 that the initial adsorption of fluoride is quite rapid. About 68%–85% of the fluoride adsorption can be achieved within the first 10 min. It can be related to the fact that at the initial stage the adsorption sites are more, and the ions can be adsorbed easily with the sites, therefore a higher adsorption rate is obtained. Moreover, the higher concentration gradient between the liquid and solid phase at the initial stage causes the higher driving force for adsorption which results in a higher adsorption rate. The slow adsorption rate in the later stage is due to the lower concentration gradient. The results are consistent with the findings of other studies [33].

### 3.3.2. Effect of pH

The effect of pH on the adsorption capacity of fluoride by modified coriander seeds was evaluated within pH ranges

of 3–11 (Fig. 5). The adsorption amount of fluoride increased from 1.7 to 2.13 mg g<sup>-1</sup> with an increase of the initial pH from 3 to 5, but it was decreased in the initial pH of 7, 9 and 11. The highest adsorption amount of fluoride (2.13 mg g<sup>-1</sup>) by modified coriander seed was obtained at pH 5.

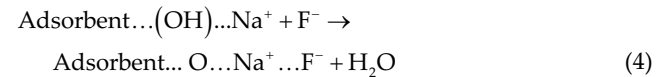
Measuring of final pH after each adsorption time (data not shown) verified that the pH of the suspension changed during adsorption. Adsorption was influenced by initial pH (pH<sub>i</sub>) and final pH (pH<sub>f</sub>) of the suspension. At low pH values, an initial pH of 3, the final pH was increased so that, the resulting values for pH<sub>i</sub>–pH<sub>f</sub> were negative. The increase of final pH at initial low pH values may be due to the occurrence of the exchange process between the adsorbent OH<sup>-</sup> and fluoride ion (Eq. (2)).



However, at the initial pH of 5 significant exchanges were not observed. At the pH range of 7–9, the pH decreased during the adsorption process leading to positive values for pH<sub>i</sub>–pH<sub>f</sub>. This is probably due to the phenomenon that Na<sup>+</sup>, liberated from NaOH used for adjusting of pH<sub>i</sub>, might have exchanged with H<sup>+</sup> which electrostatically adsorbed onto the adsorbent (Eq. (3)).



Or that may be due to the adsorption of fluoride competing with –OH ions at the secondary adsorption step where the Na<sup>+</sup> is at the first adsorption step by the adsorbent (Eq. (4)) which reduces adsorption capacity at pH<sub>i</sub> > 5.



Thus, at pH<sub>pzc</sub> less than 6.6, the adsorbent surface is protonated, resulting in a stronger electrostatic attraction between the adsorbent and fluoride ion. It should be noted that the fluoride adsorption at pH 3 is lower than that at a pH of 5. One possible reason for decreasing the adsorption of fluoride at this pH is related to the presence of fluoride ions in the form of HF. Decrease in the adsorption at pH<sub>pzc</sub> above 6.6, is due to an increase in the surface negative charges on seeds via increasing of negative groups like hydroxyl along with pH increase. The state is not suitable for the fluoride adsorption because hydroxyl ions would compete with the fluoride for the adsorption sites and also repel anionic fluoride ions [34]. In addition, at higher pH the sulfate has an important role in the fluoride adsorption, so that hydroxyl groups compete with fluoride ions for the ion exchange with sulfate. Despite the use of different adsorbent materials and modifiers in other studies, the fluctuations in fluoride adsorption influenced by pH changes has an almost similar trend with the present study [27].

### 3.3.3. Effect of adsorbent mass

The effect of adsorbent mass on the fluoride adsorption by modified coriander seeds is shown in Fig. 6. The

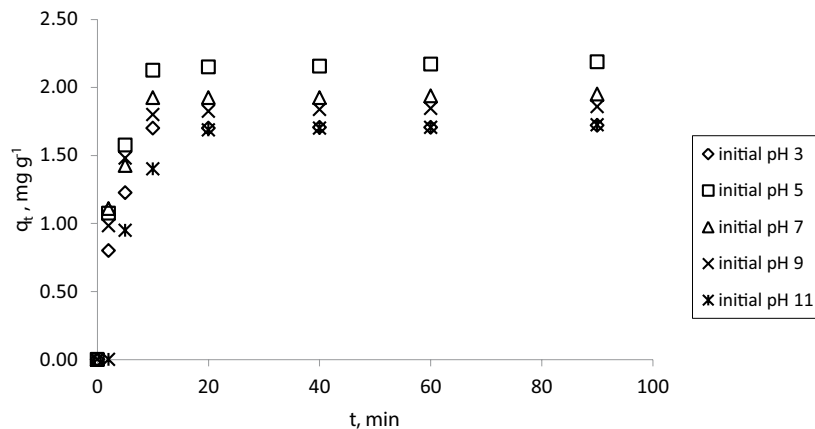


Fig. 5. Effect of initial pH on the adsorption amounts of modified coriander seeds: initial fluoride concentration, 5 mg L<sup>-1</sup>; temperature, 20°C; and adsorbent dose, 2 g L<sup>-1</sup>.

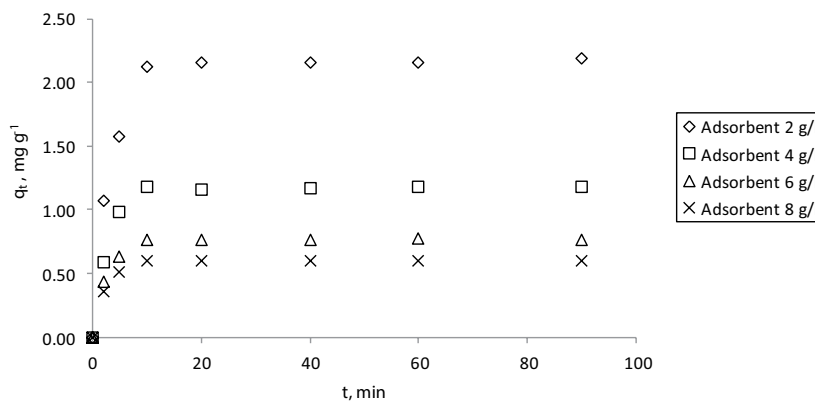


Fig. 6. Effect of adsorbent dosage on the adsorption amounts of modified coriander seeds: initial fluoride concentration, 5 mg L<sup>-1</sup>; initial pH, 5.0; and temperature, 20°C.

efficiency for fluoride removal increased with increasing of the adsorbent mass from 2 to 8 g L<sup>-1</sup>. At higher adsorbent to adsorbate concentration ratio, the adsorption rate is very fast, which results in higher removal efficiency compared to that at a lower ratio. This may be attributed to the increase in the number of adsorption sites and the availability of more sorption sites. While the amount of fluoride adsorbed per unit mass of adsorbent (adsorption capacity) decreases with the adsorbent mass increase. This is due to the split in the flux or the concentration gradient between solute in the solution and the surface of the adsorbent [35]. Moreover, the adsorption sites on the adsorbent surface remain unsaturated when the sorbent to solute concentration ratios are higher. This result was in accordance with the results of other studies [35]. When the dosage was 4 g L<sup>-1</sup>, both the removal efficiency and adsorption amount of fluoride showed high values. Therefore, the experiments were performed with an adsorbent dosage of 4 g L<sup>-1</sup>.

### 3.3.4. Effect of fluoride initial concentration and temperature

The adsorbate initial concentration plays an important role in mass transfer between the aqueous and solid phases [36,37]. The effect of initial fluoride concentration on the

rate of adsorption at different temperatures is shown in Figs. 7a–d. The curve shows that the fluoride removal varied with varying initial fluoride concentration. The removal efficiency and adsorption capacity of fluoride increased with increasing adsorption time, however, this time for different initial concentrations varied. Generally, equilibrium time increased with the increase of initial fluoride concentration (from 5 to 30 mg L<sup>-1</sup>). The adsorption amounts were greater for higher initial fluoride concentrations because the resistance to the ions adsorption is decreased by increasing the mass transfer driving force. When the initial fluoride concentration increased from 5 to 30 mg L<sup>-1</sup>, the equilibrium adsorption capacity was increased from 1.16 to 5.4 mg g<sup>-1</sup> at 20°C.

The temperature of a solution has important effects on the adsorption process [38]. Increasing the temperature reduces the viscosity of the solution, thus, the rate of diffusion of the adsorbate improves. Fig. 8 depicts the effect of temperature (10°C, 20°C, 30°C, and 40°C) which was investigated in the optimal conditions. The measurement of the kinetics of the adsorption at defined temperatures indicates an increase in the fluoride adsorption with the temperature. The results show that by increasing temperature, the required time to reach equilibrium does not change. Modeling of fluoride adsorption by modified coriander seeds can be taken

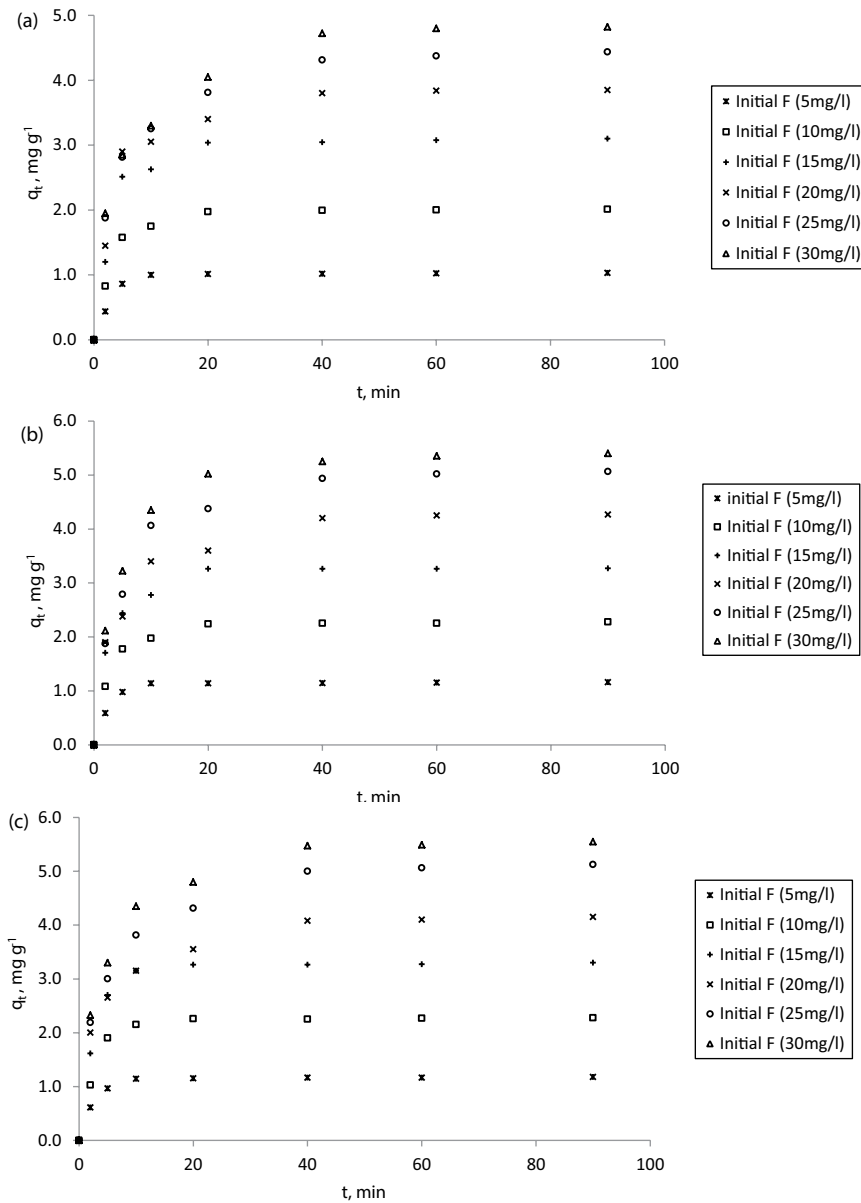


Fig. 7. Effect of the initial fluoride concentration on the adsorption amounts of modified coriander seeds at different temperature (a) 10°C, (b) 20°C, (c) 30°C, and (d) 40°C: initial fluoride concentration, 30 mg L<sup>-1</sup>; initial pH, 5.0; and adsorbent dose, 4 g L<sup>-1</sup>.

by pseudo-first-order and pseudo-second-order models. The two empirical models and description of their parameters are given in Table 1 [19,27]. The linearized forms of the models were the most used for adsorption dynamics. The pseudo-second-order can be written as [35]:

$$h = K_2 q_e^2 \tag{5}$$

The kinetic constants  $K_1$  (min<sup>-1</sup>) and  $K_2$  (min<sup>-1</sup>), the equilibrium sorption capacity  $q_e$  (mg g<sup>-1</sup>) and  $q_e^2$  (mg g<sup>-1</sup>) and also the initial sorption rate  $h$  (mg g<sup>-1</sup> min<sup>-1</sup>) based on pseudo-first and pseudo-second-order kinetics can be calculated from the plot of  $\ln(q_e - q_t)$  vs.  $t$  (Fig. 9a) and  $(t/q_t)$  vs.  $t$  (Fig. 9b), respectively.

The models' parameters, the initial sorption rate and the regression coefficients ( $R^2$ ) for the adsorption of fluoride by coriander seeds at temperatures and various initial fluoride concentrations are listed in Tables 2 and 3, respectively. Because of the lower regression coefficient value and the amount of fluoride adsorption at equilibrium determined using the pseudo-first-order model, it is obvious that this model not appropriate to the interpretation of the fluoride adsorption by coriander seeds at various initial fluoride concentrations (Table 2). The higher value of the regression coefficient for the pseudo-second-order equation suggests that it is the optimum kinetic to better understand the adsorption mechanism of fluoride on coriander seeds.

The dynamic results were correlated with the pseudo-second-order kinetic by using the non-linear curve fitting

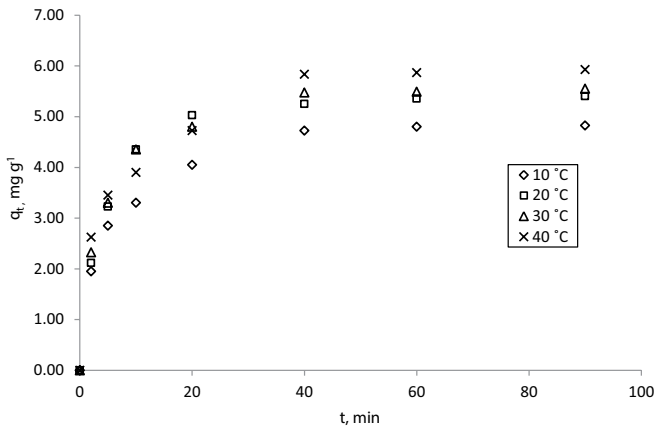


Fig. 8. Effect of temperature (a) 10°C, (b) 20°C, (c) 30°C, (d) 40°C on the fluoride uptake by modified coriander seeds: initial fluoride concentration, 30 mg L<sup>-1</sup>; initial pH, 5.0; and adsorbent dose, 4 g L<sup>-1</sup>.

analysis method and the obtained parameters are listed in Table 3. With an increase in the temperature the theoretical amount adsorbed at equilibrium, pseudo-second-order kinetic constant, and initial adsorption rate were increased (Table 2). Increasing temperature in an adsorption suspension enhances the adsorption rate due to an increase in the kinetic energy of solvent molecules. The activation energy for the adsorption of fluoride was determined by fitting the experimental data to the Arrhenius equation given below [19]:

$$K_2 = A_0 \exp\left(-\frac{E_a}{R_s T}\right) \quad (6)$$

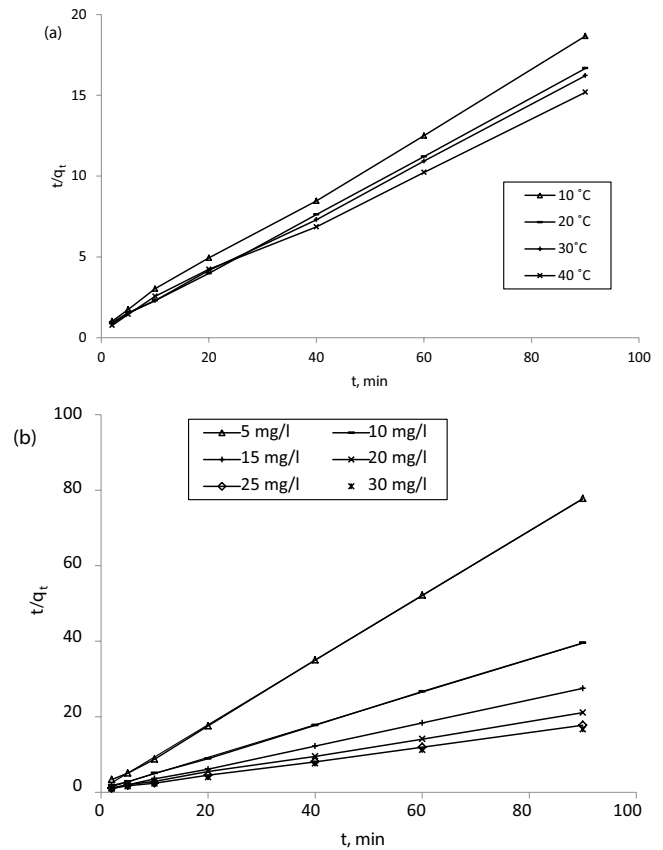


Fig. 9. (a) Pseudo-second-order adsorption kinetics at different temperature (initial pH, 5.0; initial fluoride concentration, 30 mg L<sup>-1</sup>, and adsorbent dose, 4 g L<sup>-1</sup>) and (b) at different initial concentrations (initial pH, 5.0; temperature, 20°C; and adsorbent dose, 4 g L<sup>-1</sup>).

Table 1  
Models and equations used for the description of adsorption of fluoride by coriander seeds

Model	Equation	Linear form	Description of parameters
Langmuir isotherm	$q_e = \frac{q_{max} K_L C_e}{1 + K_L C_e}$	$\frac{C_e}{q_e} = \frac{1}{q_{max} K_L} + \frac{C_e}{q_{max}}$	$q_e$ : equilibrium amount of F adsorbed per unit weight of adsorbent (mg g <sup>-1</sup> ), $q_{max}$ : the amount of F required to form monolayer (mg g <sup>-1</sup> ), $C_e$ : the equilibrium concentration of F in the solution, $K_L$ : a constant related to energy of adsorption (L mg <sup>-1</sup> ).
Freundlich isotherm	$q_e = K_F C_e^{1/n}$	$\ln q_e = \ln K_F + \frac{1}{n} \ln C_e$	$q_e$ : equilibrium amount of F adsorbed per unit weight of adsorbent (mg g <sup>-1</sup> ), $C_e$ : the equilibrium concentration of F in the solution, $K_F$ : Freundlich constant which indicates the relative adsorption capacity of the adsorbent related to bonding energy (mg g <sup>-1</sup> ), $n$ : heterogeneity factor.
Pseudo-first-order kinetic	$\frac{dq_t}{dt} = K_1 (q_e - q_t)$	$\ln(q_e - q_t) = \ln q_e - \frac{1}{n} K_1 t$	$q_e$ : equilibrium amount of F adsorbed per unit weight of adsorbent (mg g <sup>-1</sup> ), $q_t$ : amount of F adsorbed at any given time (mg g <sup>-1</sup> ) and $K_1$ : rate constant for pseudo-first-order model (min <sup>-1</sup> ).
Pseudo-second-order kinetic	$\frac{dq_t}{dt} = K_2 (q_e - q_t)^2$	$\frac{t}{q_t} = \frac{1}{K_2 q_e^2} + \frac{t}{q_e}$	$q_e$ : equilibrium amount of F adsorbed per unit weight of adsorbent (mg g <sup>-1</sup> ), $q_t$ : amount of F adsorbed at any given time (mg g <sup>-1</sup> ) and $K_2$ : rate constant for pseudo-second-order model (min <sup>-1</sup> ).

Table 2

Kinetic constants of fluoride adsorbed onto modified coriander seeds at different concentration: initial temperature 20°C, initial pH 5.0, and adsorbent dose 4 g L<sup>-1</sup>

Parameters	Fluoride concentration (mg L <sup>-1</sup> )					
	5	10	15	20	25	30
$q_{e,exp}$ (mg g <sup>-1</sup> )	1.16	2.28	3.27	4.27	5.06	5.40
Pseudo-first-order						
$K_1$ (min <sup>-1</sup> )	$31 \times 10^{-3}$	$32 \times 10^{-3}$	$46 \times 10^{-3}$	$40 \times 10^{-3}$	$33.2 \times 10^{-3}$	$33.8 \times 10^{-3}$
$q_e^1$ (mg g <sup>-1</sup> )	0.56	0.91	1.03	1.64	1.70	1.65
$R^2$	0.643	0.753	0.734	0.985	0.973	0.95
Pseudo-second-order						
$K_2$ (mg g <sup>-1</sup> min <sup>-1</sup> )	0.837	0.273	0.195	0.065	0.051	0.059
$q_e^2$ (mg g <sup>-1</sup> )	1.17	2.32	3.34	4.46	5.30	5.61
$h_0$ (mg g <sup>-1</sup> min <sup>-1</sup> )	1.15	1.47	2.18	1.28	1.43	1.86
$R^2$	0.9997	0.9998	0.9997	0.9992	0.9996	0.9998

$q_{e,exp}$ : the experimental value of  $q_e$ .

Table 3

Kinetic constants of fluoride adsorbed onto modified coriander seeds at different temperatures: initial concentrations 30 mg L<sup>-1</sup>, initial pH 5.0, and adsorbent dose 4 g L<sup>-1</sup>

Parameters	Temperature (°C)			
	10	20	30	40
$q_{e,exp}$ (mg g <sup>-1</sup> )	4.82	5.40	5.55	5.93
Pseudo-first-order				
$K_1$ (min <sup>-1</sup> )	$38 \times 10^{-3}$	$32.8 \times 10^{-3}$	$33.4 \times 10^{-3}$	$34 \times 10^{-3}$
$q_e^1$ (mg g <sup>-1</sup> )	1.77	1.65	1.72	1.90
$R^2$	0.992	0.95	0.98	0.952
Pseudo-second-order				
$K_2$ (mg g <sup>-1</sup> min <sup>-1</sup> )	$4.8 \times 10^{-2}$	$5.9 \times 10^{-2}$	$4.2 \times 10^{-2}$	$3.6 \times 10^{-2}$
$q_e^2$ (mg g <sup>-1</sup> )	5.07	5.61	5.78	6.25
$h_0$ (mg g <sup>-1</sup> min <sup>-1</sup> )	1.24	1.86	1.42	1.42
$R^2$	0.9991	0.9998	0.9996	0.9981

$q_{e,exp}$ : the experimental value of  $q_e$ .

where  $K_2$  is chemical reaction rate constant,  $A_0$  the temperature-independent factor (g mg<sup>-1</sup> min<sup>-1</sup>),  $E_a$  the activation energy (kJ mol<sup>-1</sup>),  $R_g$  the universal gas constant (8.314 J mol<sup>-1</sup> K<sup>-1</sup>) and  $T$  is the solution temperature (K). Taking the natural logarithm of Arrhenius' equation yields [19]:

$$\ln K_2 = \ln(A_0) - \frac{E_a}{R_g T} \quad (7)$$

The slope of the plot of  $\ln K_2$  vs.  $1/T$  is used to determine the activation energy (Fig. 10). The amount of  $E_a$  determines the type of adsorption, which is mainly physical or chemical. Low activation energies (5–40 kJ mol<sup>-1</sup>) indicate that the adsorption process is physical, while higher activation energies (40–800 kJ mol<sup>-1</sup>) are related to the chemical

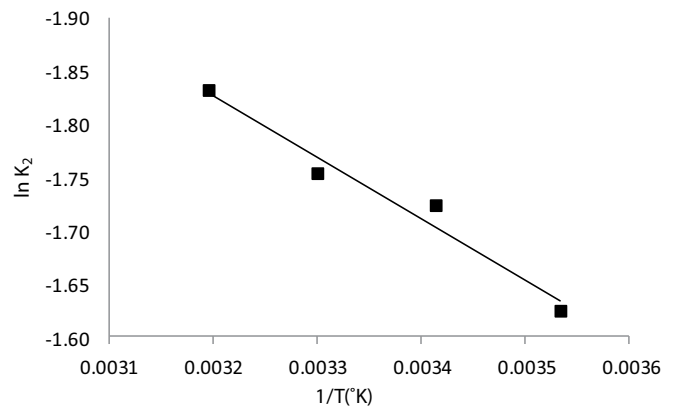


Fig. 10. The plot of pseudo-second-order kinetic constant ( $\ln K_2$ ) vs. reciprocal temperature for the adsorption of fluoride by modified coriander seeds: initial pH, 5.0 and adsorbent dose, 4 g L<sup>-1</sup>.

adsorption process [39]. The activation energy for the adsorption of fluoride on coriander seeds was 580 kJ mol<sup>-1</sup> which verifies the chemical adsorption process.

### 3.4. Thermodynamics

The efficiency of the adsorption of fluoride was investigated by the thermodynamic parameters including  $\Delta H^\circ$ ,  $\Delta G^\circ$ , and  $\Delta S^\circ$ . The value of  $\Delta G^\circ$  was obtained from the following equations [40–42]:

$$\Delta G^\circ = -RT \ln K_L \quad (8)$$

$$\ln K_L = \frac{\Delta S^\circ}{R} - \frac{\Delta H^\circ}{RT} \quad (9)$$

where  $\Delta G^\circ$  is Gibbs free energy change (J mol<sup>-1</sup>),  $\Delta S^\circ$  is entropy change (J mol<sup>-1</sup> K<sup>-1</sup>),  $\Delta H^\circ$  is enthalpy change (J mol<sup>-1</sup>),  $R$  is the ideal gas constant (8.314 J K<sup>-1</sup> mol<sup>-1</sup>), and  $T$  is the reaction temperature (Kelvin).

Thermodynamic parameters for fluoride removal onto modified coriander seeds are shown in Table 4. As shown in the table,  $\Delta G^\circ$  of fluoride adsorbing onto modified coriander seeds at the temperature 283 K was positive, but the  $\Delta G^\circ$  was negative at temperatures 293, 303 and 313 K, so the adsorption process of fluoride onto modified coriander seeds was a spontaneous process at 293, 303 and 313 K, and a non-spontaneous process at 283 K. Additionally, the findings illustrated that  $\Delta H^\circ$  was positive, which demonstrates that the adsorption process is endothermic, so an increase of temperature results in more fluoride ion adsorption. Furthermore, positive  $\Delta S^\circ$  values were obtained, which indicates an increase in randomness at the solid-solution interface during the adsorption of fluoride onto the adsorbent.

### 3.5. Adsorption isotherms

The adsorption isotherms are key parameters for designing adsorption systems. Fitting of the isotherm data to different isotherm models is a basic step to select a suitable model used for design purposes. The adsorption isotherm interprets how the adsorbate distributes between liquid and solid phase when the adsorption process reaches an equilibrium state. Several equilibrium models have been developed to describe adsorption isotherm that the Langmuir and Freundlich equations are the most used models [18,43]. In this study, we analyzed the adsorption data with both Langmuir and Freundlich isotherm models. The equations of the models and the linear forms used to calculate the model parameters are explained in Table 1

Table 4  
Thermodynamic parameters for fluoride removal onto modified coriander seeds

Adsorbent	Temperature (K)	$\Delta G^\circ$ (kJ mol <sup>-1</sup> )	$\Delta H^\circ$ (kJ mol <sup>-1</sup> )	$\Delta G^\circ$ (kJ mol <sup>-1</sup> K <sup>-1</sup> )	$R^2$
Modified coriander seeds	283	2.14	119.33	0.077	0.97
	293	-0.05			
	303	-3.15			
	313	-4.44			

Table 5  
Adsorption isotherm parameters for the adsorption of fluoride onto modified coriander seeds at different temperatures: initial concentration 30 mg L<sup>-1</sup>, initial pH 5.0, and adsorbent dose 4 g L<sup>-1</sup>

Parameters	Temperature (°C)			
	10	20	30	40
<b>Langmuir isotherm</b>				
$q_m$ (mg g <sup>-1</sup> )	9.48	6.62	5.76	6.01
$K_L$ (L mg <sup>-1</sup> )	0.14	0.57	0.84	0.964
$R^2$	0.984	0.999	0.992	0.9873
$R_L$	0.190–0.585	0.055–0.259	0.038–0.193	0.033–0.172
<b>Freundlich isotherm</b>				
$K_F$ (L mg <sup>-1</sup> )	0.13	0.34	0.36	0.41
$n$	1.63	1.98	2.05	1.96
$R^2$	0.918	0.954	0.980	0.987

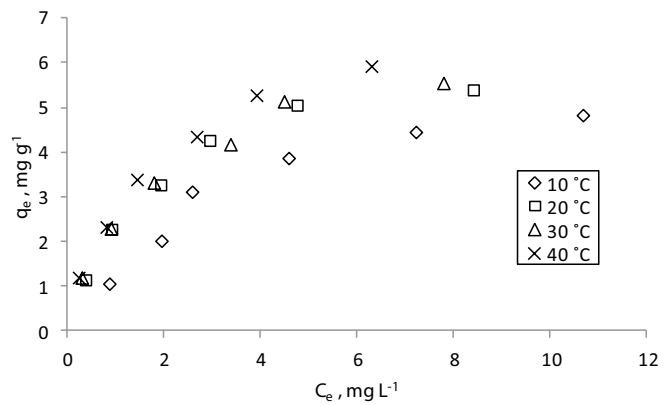


Fig. 11. Equilibrium isotherms of fluoride adsorption by modified coriander seeds at different temperatures: adsorption time, 90 min; initial pH, 5.0; and adsorbent dose, 4 g L<sup>-1</sup>.

[27]. The linear forms are used to determine the best-fitting isotherm for both models.

Isotherm data showed that the amount of fluoride adsorption increased with increasing initial fluoride concentration from 5 to 30 mg L<sup>-1</sup>. Fig. 11 shows the amount of fluoride adsorbed at 10°C, 20°C, 30°C and 40°C plotted vs. its equilibrium concentration in the aqueous phase. The amount of fluoride adsorption increased by increasing the temperature from 10°C to 40°C. The calculated Langmuir and Freundlich isotherm constants for the adsorption at different temperatures are listed in Table 5. By comparing the linear regression values ( $R^2$ ), it is clear that

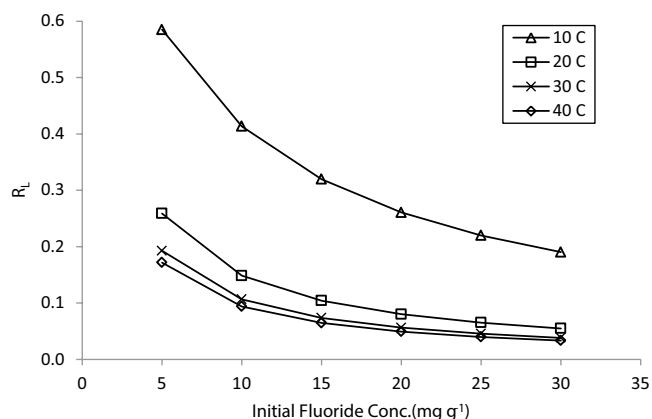


Fig. 12. Separation factor for fluoride adsorption by modified coriander seeds at various temperatures: adsorption time, 90 min; initial pH, 5.0; and adsorbent dose, 4 g L<sup>-1</sup>.

at all temperatures the adsorption data is compatible with both the Langmuir and Freundlich isotherms. The experimental data were best adjusted to these both models, based on  $R^2$  values, it indicates that the material is homogeneous.

The type of the Langmuir isotherm can be predicted whether the adsorption is favorable or unfavorable. It can be determined by a dimensionless constant separation factor,  $R_L$ , which is defined by Eq. (10) [35]:

$$R_L = \frac{1}{1 + K_L C_0} \quad (10)$$

where  $C_0$  (mg L<sup>-1</sup>) is the initial concentration of adsorbate. The parameter  $R_L$  indicates the shape of isotherm as follows:  $R_L > 1$ , unfavorable;  $R_L = 1$ , linear;  $0 < R_L < 1$ , favorable;  $R_L = 0$ , irreversible. The  $R_L$  values obtained for the fluoride adsorbed onto modified coriander seeds were between 0 and 1, which confirms a highly favorable adsorption (Fig. 12). A comparison of the fluoride removal efficiency of different sorbents is given in Table 6.

### 3.6. Regeneration and reusability study

The effect of the regeneration of modified coriander seeds was studied in batch adsorption tests. Four regeneration cycles were considered to know the adsorption efficiency of fluoride. 30 mg L<sup>-1</sup> fluoride concentration was taken, and then an adsorbent dose 4 g L<sup>-1</sup> was added and vigorously stirred in NaOH for 90 min. Further, it was filtered and the residual concentration of fluoride was determined. After that, the adsorbent was dried and used again in the next cycles. The removal efficiency of fluoride in cycle 1, 2, 3 and 4 was 90%, 82%, 70%, 65%, respectively.

## 4. Conclusions

This study showed that the modified coriander seeds can be a suitable adsorbent for the separation of fluoride ion from water due to its attractive features such as high efficiency and rate of adsorption, nontoxic, low expense and reusability. The maximum adsorption capacity can be

Table 6  
Comparison of the fluoride removal efficiency of different sorbents

Adsorbent	Adsorption capacity (mg g <sup>-1</sup> )	Reference
Activated charcoal	1.076	[44]
Tea leaves biomass	0.054	[45]
Thermally activated carbon	4.617	[46]
Tamarind seed biosorbent	6.37	[47]
<i>Phyllanthus emblica</i> activated carbon	7.172	[48]
Lanthanum-incorporated chitosan beads	4.7	[49]
Chitosan iron complex	2.3	[50]
Eucalyptus leaves modified with ZnCl <sub>2</sub>	3.5	[51]
Banana peel	2.283	[52]
Groundnut shell	3.344	[52]
Sweet lemon peel	1.037	[52]
Fungal biomass ( <i>Pleurotus ostreatus</i> 1804)	1.272	[53]
<i>Eichhornia crassipes</i> biomass and its carbonized form	0.523–1.54	[54]
Zirconium impregnated coconut shell carbon	6.41	[55]
Waste carbon slurry	4.306	[56]
Zr(IV)-loaded grape pomace (Zr(IV)-GP) biosorbent	7.54	[57]
Modified native cellulose	8.55	[57]
Al-Zr impregnated cellulose	2.40	[57]
Chitin-based biocomposite	0.29	[58]
Modified coriander seeds	6.01	Current study

achievable at a high initial concentration of fluoride. The results indicated that the sorption process is influenced by adsorption parameters such as contact time, initial pH, adsorbent dosage, initial fluoride concentration, and temperature. The regression coefficients obtained from the isotherms models represented that the Langmuir model has the best fit to the adsorption data. Based on the kinetic studies, the pseudo-second-order model yielded a better fit to experimental data, showing a chemisorption process. The adsorption process of fluoride removal onto modified coriander seeds was endothermic. Therefore, the adsorbent can be proposed for the removal of fluoride from aqueous solution.

## Acknowledgment

The authors wish to thank the Department of Environmental Health Engineering, Ardebil University of Medical Sciences, for financial support and providing research facilities.

## References

- [1] M. Qasemi, M. Afsharnia, M. Farhang, A. Bakhshizadeh, M. Allahdadi, A. Zarei, Health risk assessment of nitrate exposure in groundwater of rural areas of Gonabad and Bajestan, Iran, *Environ. Earth Sci.*, 77 (2018) 551.
- [2] M. Yousefi, S. Ghalehaskar, F.B. Asghari, A. Ghaderpoury, M.H. Dehghani, M. Ghaderpoori, A.A. Mohammadi, Distribution of fluoride contamination in drinking water resources and health risk assessment using geographic information system, northwest Iran, *Regul. Toxicol. Pharm.*, 107 (2019) 104408.
- [3] F. Shen, X. Chen, P. Gao, G. Chen, Electrochemical removal of fluoride ions from industrial wastewater, *Chem. Eng. Sci.*, 58 (2003) 987–993.
- [4] G. De la Puente, J. Pis, J. Menéndez, P. Grange, Thermal stability of oxygenated functions in activated carbons, *J. Anal. Appl. Pyrolysis*, 43 (1997) 125–138.
- [5] A. Vázquez-Guerrero, R. Alfaro-Cuevas-Villanueva, J.G. Rutiaga-Quiñones, R. Cortés-Martínez, Fluoride removal by aluminum-modified pine sawdust: effect of competitive ions, *Ecol. Eng.*, 94 (2016) 365–379.
- [6] Y. Zhang, Y. Hu, N. Sun, S.A. Khoso, L. Wang, W. Sun, A novel precipitant for separating lithium from magnesium in high Mg/Li ratio brine, *Hydrometallurgy*, 187 (2019) 125–133.
- [7] N. Reddy, K. Prasad, Pyroclastic fluoride in ground waters in some parts of Tadpatri Taluk, Anantapur district, Andhra Pradesh, *Indian J. Environ. Health*, 45 (2003) 285–288.
- [8] M. Ghaderpoori, G.R.J. Khaniki, M. Dehghani, M. Shams, A. Zarei, Determination of fluoride in bottled water sold in Tehran market, Iran, *Am. Eurasian J. Agric. Environ. Sci.*, 6 (2009) 324–327.
- [9] Y. Yu, C. Wang, X. Guo, J.P. Chen, Modification of carbon derived from *Sargassum* sp. by lanthanum for enhanced adsorption of fluoride, *J. Colloid Interface Sci.*, 441 (2015) 113–120.
- [10] P.T. Harrison, Fluoride in water: a UK perspective, *J. Fluorine Chem.*, 126 (2005) 1448–1456.
- [11] A. García-Pérez, M. Irigoyen-Camacho, A. Borges-Yáñez, Fluorosis and dental caries in Mexican schoolchildren residing in areas with different water fluoride concentrations and receiving fluoridated salt, *Caries Res.*, 47 (2013) 299–308.
- [12] WHO, Guidelines for Drinking-Water Quality, Recommendations, World Health Organization, Geneva, 2004.
- [13] A. Tressaud, *Advances in Fluorine Science, Fluorine and the Environment, Agrochemicals, Archaeology, Green Chemistry & Water*, Elsevier, Oxford, UK, 2 (2006) 1–286.
- [14] S. Ayoob, A. Gupta, V.T. Bhat, A conceptual overview on sustainable technologies for the defluoridation of drinking water, *Crit. Rev. Env. Sci. Technol.*, 38 (2008) 401–470.
- [15] P. Miretzky, A.F. Cirelli, Fluoride removal from water by chitosan derivatives and composites: a review, *J. Fluorine Chem.*, 132 (2011) 231–240.
- [16] H. Hu, L. Yang, Z. Lin, X. Xiang, X. Jiang, L. Hou, Preparation and characterization of novel magnetic Fe<sub>3</sub>O<sub>4</sub>/chitosan/Al(OH)<sub>3</sub> beads and its adsorption for fluoride, *Int. J. Biol. Macromol.*, 114 (2018) 256–262.
- [17] R. Khosravi, A. Zarei, M. Heidari, A. Ahmadfazel, M. Vosoghi, M. Fazlzadeh, Application of ZnO and TiO<sub>2</sub> nanoparticles coated onto montmorillonite in the presence of H<sub>2</sub>O<sub>2</sub> for efficient removal of cephalexin from aqueous solutions, *Korean J. Chem. Eng.*, 35 (2018) 1000–1008.
- [18] R. Khosravi, H. Eslami, A. Zarei, M. Heidari, A.N. Baghani, N. Safavi, A. Mokammel, M. Fazlzadeh, S. Adhami, Comparative evaluation of nitrate adsorption from aqueous solutions using green and red local montmorillonite adsorbents, *Desal. Wat. Treat.*, 116 (2018) 119–128.
- [19] K. Biswas, K. Gupta, U.C. Ghosh, Adsorption of fluoride by hydrous iron(III)-tin(IV) bimetal mixed oxide from the aqueous solutions, *Chem. Eng. J.*, 149 (2009) 196–206.
- [20] M. Bhatnagar, A. Bhatnagar, S. Jha, Interactive biosorption by microalgal biomass as a tool for fluoride removal, *Biotechnol. Lett.*, 24 (2002) 1079–1081.
- [21] R.K. Bharali, K.G. Bhattacharyya, Biosorption of fluoride on neem (*Azadirachta indica*) leaf powder, *J. Environ. Chem. Eng.*, 3 (2015) 662–669.
- [22] S. Manikandan, S. Chidambaram, A. Ramanathan, M.V. Prassanna, U. Karmegam, C. Singaraja, P. Paramaguru, I. Jainab, A study on the high fluoride concentration in the magnesium-rich waters of hard rock aquifer in Krishnagiri district, Tamilnadu, India, *Arabian J. Geosci.*, 7 (2014) 273–285.
- [23] S. Bhat, P. Kaushal, M. Kaur, H. Sharma, Coriander (*Coriandrum sativum* L.): processing, nutritional and functional aspects, *Afr. J. Plant Sci.*, 8 (2014) 25–33.
- [24] I. Gaballah, D. Goy, E. Allain, G. Kilbertus, J. Thauront, Recovery of copper through decontamination of synthetic solutions using modified barks, *Metall. Mater. Trans. B*, 28 (1997) 13–23.
- [25] A. Özer, D. Özer, A. Özer, The adsorption of copper (II) ions on to dehydrated wheat bran (DWB): determination of the equilibrium and thermodynamic parameters, *Process Biochem.*, 39 (2004) 2183–2191.
- [26] APHA, 22nd ed., E.W. Rice, R.B. Baird, A.D. Eaton, L.S. Clesceri, Standard Methods for the Examination American Public Health Association (APHA), Washington, D.C., 2012.
- [27] T. Nur, P. Loganathan, T. Nguyen, S. Vigneswaran, G. Singh, J. Kandasamy, Batch and column adsorption and desorption of fluoride using hydrous ferric oxide: solution chemistry and modeling, *Chem. Eng. J.*, 247 (2014) 93–102.
- [28] M. Qasemi, A. Zarei, M. Afsharnia, R. Salehi, M. Allahdadi, M. Farhang, Data on cadmium removal from synthetic aqueous solution using garbage ash, *Data Brief*, 20 (2018) 1115–1123.
- [29] H. Sadek, A. Helmy, V. Sabet, T.F. Tadros, Adsorption of potential-determining ions at the aluminium oxide-aqueous interface and the point of zero charge, *J. Electroanal. Chem. Interfacial Electrochem.*, 27 (1970) 257–266.
- [30] A. Bhatnagar, E. Kumar, M. Sillanpää, Fluoride removal from water by adsorption—a review, *Chem. Eng. J.*, 171 (2011) 811–840.
- [31] S.S. Tripathy, J.-L. Bersillon, K. Gopal, Removal of fluoride from drinking water by adsorption onto alum-impregnated activated alumina, *Sep. Purif. Technol.*, 50 (2006) 310–317.
- [32] D. Pavia, G. Lampman, G. Kriz, J. Vyvyan, *Introduction to Spectroscopy* Cengage Learning, Ainara López Maestresalas, 2008.
- [33] S. Zhang, Y. Lu, X. Lin, X. Su, Y. Zhang, Removal of fluoride from groundwater by adsorption onto La(III)-Al(III) loaded scoria adsorbent, *Appl. Surf. Sci.*, 303 (2014) 1–5.
- [34] D. Thakre, S. Jagtap, N. Sakhare, N. Labhsetwar, S. Meshram, S. Rayalu, Chitosan based mesoporous Ti-Al binary metal oxide supported beads for defluoridation of water, *Chem. Eng. J.*, 158 (2010) 315–324.
- [35] L. Nouri, I. Ghodbane, O. Hamdaoui, M. Chiha, Batch sorption dynamics and equilibrium for the removal of cadmium ions from aqueous phase using wheat bran, *J. Hazard. Mater.*, 149 (2007) 115–125.
- [36] M.H. Dehghani, M. Farhang, M. Alimohammadi, M. Afsharnia, G. McKay, Adsorptive removal of fluoride from water by activated carbon derived from CaCl<sub>2</sub>-modified *Crocus sativus* leaves: equilibrium adsorption isotherms, optimization, and influence of anions, *Chem. Eng. Commun.*, 205 (2018) 955–965.
- [37] M.H. Dehghani, A. Zarei, A. Mesdaghinia, R. Nabizadeh, M. Alimohammadi, M. Afsharnia, G. McKay, Production and application of a treated bentonite–chitosan composite for the efficient removal of humic acid from aqueous solution, *Chem. Eng. Res. Des.*, 140 (2018) 102–115.
- [38] A.A. Mohammadi, A. Zarei, H. Alidadi, M. Afsharnia, M. Shams, Two-dimensional zeolitic imidazolate framework-8 for efficient removal of phosphate from water, process modeling, optimization, kinetic, and isotherm studies, *Desal. Wat. Treat.*, 129 (2018) 244–254.
- [39] H. Nollet, M. Roels, P. Lutgen, P. Van der Meeren, W. Verstraete, Removal of PCBs from wastewater using fly ash, *Chemosphere*, 53 (2003) 655–665.
- [40] Y. Li, Q. Du, T. Liu, J. Sun, Y. Jiao, Y. Xia, L. Xia, Z. Wang, W. Zhang, K. Wang, Equilibrium, kinetic and thermodynamic studies on the adsorption of phenol onto graphene, *Mater. Res. Bull.*, 47 (2012) 1898–1904.

- [41] S. Dehghanpour, A. Mahmoudi, F. Esbati, Surfactant-assistant solvo/hydrothermal methods for preparation of nanoscale calcium aminodiphosphonates exhibiting high methylene blue adsorption affinity, *Mater. Res. Bull.*, 47 (2012) 2126–2134.
- [42] A. Štrkalj, J. Malina, Thermodynamic and kinetic study of adsorption of Ni (II) ions on carbon anode dust, *Chem. Eng. Commun.*, 198 (2011) 1497–1504.
- [43] M. Qasemi, M. Afsharnia, A. Zarei, A.A. Najafpoor, S. Salari, M. Shams, Phenol removal from aqueous solution using *Citrullus colocynthis* waste ash, *Data Brief*, 18 (2018) 620–628.
- [44] A. Tembhurkar, S. Dongre, Studies on fluoride removal using adsorption process, *J. Environ. Sci. Eng.*, 48 (2006) 151–156.
- [45] G. Munavalli, V. Patki, A comparative study of defluoridation techniques, *J IPHE, India*, 10 (2009) 35–34.
- [46] G. Alagumuthu, V. Veeraputhiran, R. Venkataraman, Adsorption isotherms on fluoride removal: batch techniques, *Arch. Appl. Sci. Res.*, 2 (2010) 170–185.
- [47] M. Murugan, E. Subramanian, Studies on defluoridation of water by Tamarind seed, an unconventional biosorbent, *J. Water Health*, 4 (2006) 453–461.
- [48] V. Veeraputhiran, G. Alagumuthu, Sorption equilibrium of fluoride onto *Phyllanthus emblica* activated carbon, *Int. J. Res. Chem. Environ.*, 1 (2011) 42–47.
- [49] A. Teutli-Sequeira, M. Solache-Ríos, V. Martínez-Miranda, I. Linares-Hernández, Comparison of aluminum modified natural materials in the removal of fluoride ions, *J. Colloid Interface Sci.*, 418 (2014) 254–260.
- [50] Y. Hu, H. Kazemian, S. Rohani, Y. Huang, Y. Song, In situ high pressure study of ZIF-8 by FTIR spectroscopy, *Chem. Commun.*, 47 (2011) 12694–12696.
- [51] E. Bazrafshan, N. Khoshnamvand, A.H. Mahvi, Fluoride removal from aqueous environments by ZnCl<sub>2</sub>-treated eucalyptus leaves as a natural adsorbent, *Fluoride*, 48 (2015) 315–320.
- [52] A. Mohammad, C. Majumder, Removal of fluoride from synthetic waste water by using “bio-adsorbents”, *Int. J. Res. Eng. Technol.*, 3 (2014) 776–785.
- [53] S. Ramanaiah, S.V. Mohan, P. Sarma, Adsorptive removal of fluoride from aqueous phase using waste fungus (*Pleurotus ostreatus* 1804) biosorbent: kinetics evaluation, *Ecol. Eng.*, 31 (2007) 47–56.
- [54] S. Sinha, K. Pandey, D. Mohan, K.P. Singh, Removal of fluoride from aqueous solutions by *Eichhornia crassipes* biomass and its carbonized form, *Ind. Eng. Chem. Res.*, 42 (2003) 6911–6918.
- [55] R.S. Sathish, N. Raju, G. Raju, G. Nageswara Rao, K.A. Kumar, C. Janardhana, Equilibrium and kinetic studies for fluoride adsorption from water on zirconium impregnated coconut shell carbon, *Sep. Sci. Technol.*, 42 (2007) 769–788.
- [56] V.K. Gupta, I. Ali, V.K. Saini, Defluoridation of wastewaters using waste carbon slurry, *Water Res.*, 41 (2007) 3307–3316.
- [57] Y. Zhang, K. Huang, Grape pomace as a biosorbent for fluoride removal from groundwater, *RSC Adv.*, 9 (2019) 7767–7776.
- [58] J.L. Davila-Rodriguez, V.A. Escobar-Barrios, K. Shirai, J.R. Rangel-Mendez, Synthesis of a chitin-based biocomposite for water treatment: optimization for fluoride removal, *J. Fluorine Chem.*, 130 (2009) 718–726.